Study of polarization observables in double pion photoproduction on the proton

J.C. Nacher and E. Oset

Departamento de Física Teórica and IFIC

Centro Mixto Universidad de Valencia-CSIC

Institutos de Investigación de Paterna, Apdo. correos 22085,

46071, Valencia, Spain

Abstract

Using a model for two pion photoproduction on the proton previously tested in total cross sections and invariant mass distributions, we evaluate here polarization observables on which recent experiments are providing new information. We evaluate cross sections for spin 1/2 and 3/2, which are measured at Mainz and play an important role in tests of the GHD sum rule. We also evaluate the proton polarization asymmetry Σ which is currently under investigation at GRAAL in Grenoble.

1 Introduction

Photoproduction of two pions has been the object of intense recent experimental [1, 2, 3, 4, 5] and theoretical work [6, 7, 8, 9, 10, 11]. The data are very sensitive to couplings of resonances to photons and mesons and in particular are a unique source of information on the $N^*(1520) \rightarrow \Delta\pi$ transition which can be contrasted with quark model predictions [12].

The total cross sections and invariant mass distributions bare much information on the reaction mechanisms and they pose important constraints on the theoretical models. Yet, further constraints are to be found in the polarization observables and so far the theoretical models have not tackled this problem. The advent of recent experiments on this issue makes the theoretical problem opportune. Furthermore the spin 1/2 and 3/2 γp cross sections are input for the Drell-Gerasimov-Hearm sum rule, which is also receiving much attention recently [13, 15]. Given the fact that the photonuclear excitation of the proton gives rise to a rich spectrum of resonances in the $1-2$ GeV region, the DGH sum rule establishes an interesting link between a static property of the nucleon and the dynamical mechanisms of the nucleon excitation.

The sum rule was first derived by Gerasimov and by Drell and Hearn in an independent way and it is based on the work of the Low Energy Theorem of Low and Gell-Mann and Goldberger for spin 1/2 particles.

The most important fact of this relation lies in the fact that it is based on general principles as Gauge and Lorentz invariance, cross symmetry, causality and unitarity. However, testing the DGH sum rule has proved so far problematic for lack of data at high energies. This handicap has been overcome by using theoretical predictions for the one pion photoproduction [13]. However, since one also needs the two pion production cross section, the use of theoretical models to evaluate the contribution of this part becomes also necessary.

At the moment the rough estimates of [14] are used in the test of the DGH sum rule, but the existence of fair models for two pion photoproduction makes the evaluation of the spin cross sections needed in the DGH test most advisable. In fact, lack of data or theoretical predictions for the two pion production on deuterium was the reason in [15] to stop the integration at the value of 550 MeV before the two pion production becomes relevant.

The recent measurement of the helicity 1/2, 3/2 cross sections in two pion photoproduction at Mainz [16] represents an important step in the test of the DGH sum rules while at the same time it imposes new constraints on the theoretical models of two pion photoproduction. The present status of the theory has also experienced a step forward with the solving of the puzzle of the $\gamma p \rightarrow n\pi^+\pi^0$ cross section which was underpredicted in [6, 8]. The inclusion of the $\Delta(1700)$ excitation, together with ρ production, lead in [17] to good predictions for cross sections and invariant mass distributions of the $\gamma p \rightarrow n\pi^+\pi^0$ reaction, without spoiling the agreement found for the other charge channels. The model of [17] seems thus most suited to evaluate the spin cross sections, hence serving the double purpose of further testing model, while at the same time, using it as input to test the GDH sum rule.

Additionally more polarization observables, like the polarization asymmetry Σ are been measured in the European detector GRAAL at Grenoble. The perfect cylindrical symmetry of the GRAAL detector is ideal to measure Σ. Up to now the GRAAL collaboration has presented results for only one emitted meson in the final state [18] but recently preliminary results for the Σ in the $\gamma p \to \pi^0\pi^0 p$, $\gamma p \to \pi^+\pi^- p$ and $\gamma p \to \pi^+\pi^0 n$ channels are in progress in the range of photon energies 500-1100 MeV [19].

With all this information ready to appear in experimental publications in a short time we will use our two pion photoproduction model to analyze the observables described above which pose a new challenge to the model.

2 Helicity asymmetries for $\gamma p \to \pi^+\pi^- p$ and $\gamma p \to \pi^+\pi^0 n$

The helicity cross sections $\sigma_{3/2}$ ($\sigma_{1/2}$) are defined as the total cross section for the absorption of a circularly polarized photon by a proton polarized with its spin parallel (anti parallel) to the photon spin.

The polarization vectors for circularly polarized photons are :

$$\vec{\epsilon}^{\,(\pm)} = \frac{(\mp 1, -i, 0)}{\sqrt{2}} \tag{1}$$

By writing our $\gamma p \to \pi\pi N$ amplitude as $\epsilon_\mu T^\mu$, we evaluate the amplitudes for scattering of the polarized photon with a proton with spin third component 1/2. Then we have the $T_{1/2}$ and $T_{3/2}$ helicity amplitudes as:

$$T_{3/2} = \frac{-T^x - iT^y}{\sqrt{2}}\,, \tag{2}$$

$$T_{1/2} = \frac{T^x - iT^y}{\sqrt{2}}\,. \tag{3}$$

Alternatively, we could also use the photon with $\vec{\epsilon}^{\,(+)}$ polarization and third components 1/2 or $-1/2$ for the proton spin, as is customarily done to define helicity amplitudes of resonances. For a N^* resonance the helicity amplitudes $A_{1/2}$ and $A_{3/2}$ are defined as

$$A^{N^*}_{1/2} \sim \langle N^*, J_z = 1/2 | \vec{\epsilon}^{\,(+)} \cdot \vec{J} | N, S_z = -1/2 \rangle \tag{4}$$

$$A^{N^*}_{3/2} \sim \langle N^*, J_z = 3/2 | \vec{\epsilon}^{\,(+)} \cdot \vec{J} | N, S_z = 1/2 \rangle \tag{5}$$

In these cases $A_{1/2}$ means an incoming nucleon with spin projection $S_z = -\frac{1}{2}$ (positive helicity) absorbing a photon with spin $\lambda = +1$, leading to $J_z = \frac{1}{2}$ for the resonance final state (same helicity as in initial state). For the case of the $A_{3/2}$ it means that we have an initial nucleon spin projection state of $S_z = \frac{1}{2}$ (negative helicity) and a photon with $\lambda = +1$, being the final spin state $J_z = 3/2$ (positive helicity, helicity change).

As we said in the Introduction, experiments about that kind of observables and being performed with the DAPHNE detector at Mainz. The DAPHNE angular acceptance for the two charged pion production in the GDH-Experiment at MAMI for hydrogen target and butanol target is defined as [16]

Polar angle(θ): $23 \leq \theta \leq 158$ [deg]

Azimuthal angle(ϕ): $0 \leq \phi \leq 360(2\pi)$ [deg]

For the $\gamma p \to \pi^+\pi^- p$ reaction they can see up to three charged particles inside the DAPHNE-detector. Depending upon the number of the particles seen, it is necessary to apply different methods of analysis which affect the DAPHNE-acceptance for this reaction. The number of particles has to be handled as follows:

i) 0 and 1 charged particle in the DAPHNE angular acceptance:

The events gets rejected.

ii) 2 charged particle in the DAPHNE angular acceptance

There are two possible sets of particles that can be seen by the DAPHNE detector in such a case, which are $(p^{\pm}_{\pi})$ or $(\pi^+\pi^-)$.

iii) 3 charged particle in DAPHNE angular acceptance:

In this case the proton momentum threshold $(p_{prot}/(MeV/c))$ against the polar angle (θ /degrees) is specified by the following function:

$$P_{prot}(threshold) > 300 + 0.010(\theta - 90)^2 \, [MeV/c] \,, \tag{6}$$

and the charged pion (π^+, π^-) momentum threshold ($p_{\pi^\pm}$ /(MeV/c)) against the polar angle (θ /degrees) is specified by:

$$p_{\pi^\pm} > 65 + 0.005(\theta - 90)^2 \, [MeV/c] \,. \tag{7}$$

We adapt our calculations to the $\gamma p \to \pi^+\pi^- p$ reactions are to the experimental acceptance discussed above for the three particle detection case. In our calculations we use the improved model for two pion photoproduction mentioned in the introduction [17]. We analyze the $\sigma_{1/2}$, $\sigma_{3/2}$ observables and the helicity asymmetry in the following figures.

In fig. 1 we show the $\sigma_{3/2}$ and $\sigma_{1/2}$ cross sections for the $\vec{\gamma}\vec{p} \to p\pi^+\pi^-$ reaction with the 3 charged particles in the DAPHNE acceptance. We see that the agreement with the experimental points is quite good for $\sigma_{1/2}$ and $\sigma_{3/2}$. We reproduce a peak around 700 MeV shown by the experimental data. We see a small discrepancy with the experiment at photon energies up to 700 MeV but the decrease of the cross section up 800 MeV is reproduced.

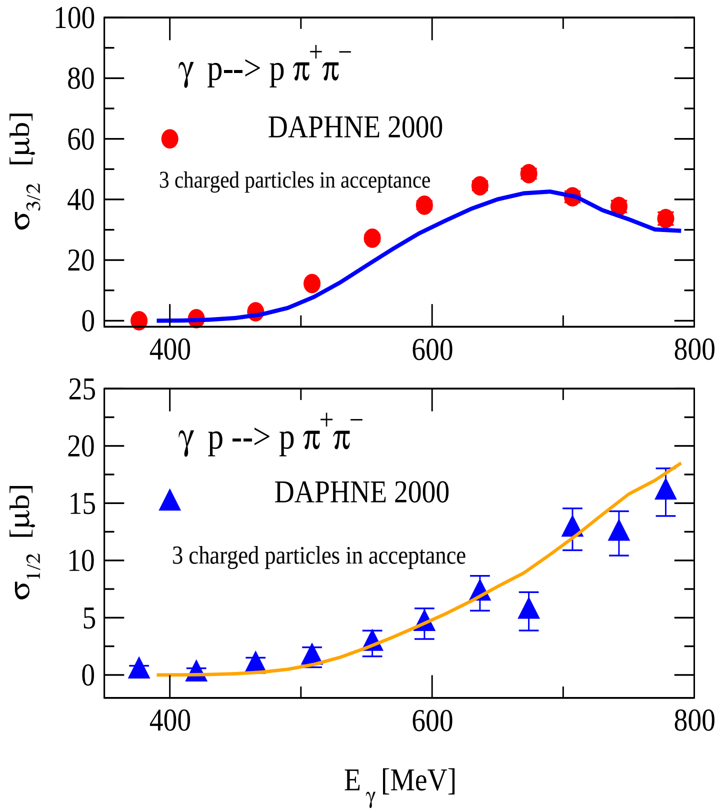

Figure 1: $\sigma_{3/2}$, $\sigma_{1/2}$ for $\vec{\gamma}\vec{p} \to p\pi^+\pi^-$ with 3 charged particles in DAPHNE acceptance. Experimental data from [16]

In fig. 2 we show the difference between the helicity cross sections $\sigma_{3/2}$ and $\sigma_{1/2}$ at the top of the figure. In the bottom we show the helicity asymmetry for the double charged pion reaction with 3 particles in the DAPHNE acceptance. We find a similar result for the $\sigma_{3/2}$-$\sigma_{1/2}$ cross section as we showed before for the $\sigma_{3/2}$, reflecting the dominance of the helicity amplitude $A_{3/2}$. The helicity asymmetry is defined by $\frac{\sigma_{3/2}-\sigma_{1/2}}{\sigma_{3/2}+\sigma_{1/2}}$ and we observe a nice agreement with the experimental data although one has large experimental error bars at low and high energy.

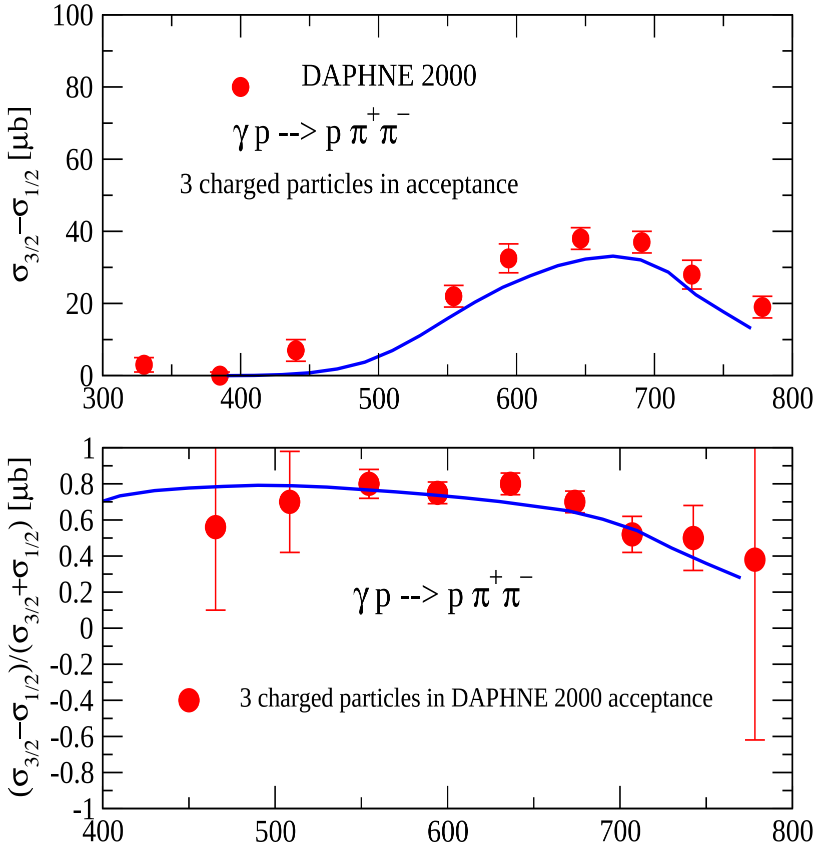

Figure 2: The difference of cross sections, $\sigma_{3/2}$ - $\sigma_{1/2}$, for the $\vec{\gamma}\vec{p} \to p\pi^+\pi^-$ reaction with 3 charged particles in DAPHNE acceptance, is shown in the top figure and the helicity asymmetry in the bottom one. Experimental data from [16]

We turn now to the $\vec{\gamma}\vec{p} \to \pi^+\pi^0 n$ reaction. In our work [17] we added to the model some new ingredients improving considerably the results for the $\gamma p \to n\pi^+\pi^0$ channel obtained before in [8]. We shall show now the results of this channel for the helicity observables analyzed above.

The DAPHNE acceptance for $n\pi^+\pi^0$ is as follows: the n and π^0, both have no limits in angular acceptance and in threshold momentum. Only the π^+ is limited by the angle and momentum threshold. So, in the $\gamma p \to n\pi^+\pi^0$ reaction we should take the π^+ inside the DAPHNE acceptance. In this case there is a threshold for the momentum of the charged pion given as a function of the polar angle ($\theta/degrees$) by:

$$p_{\pi^+} > 80 + 0.005(\theta - 90)^2 \, [MeV/c] \quad (8)$$

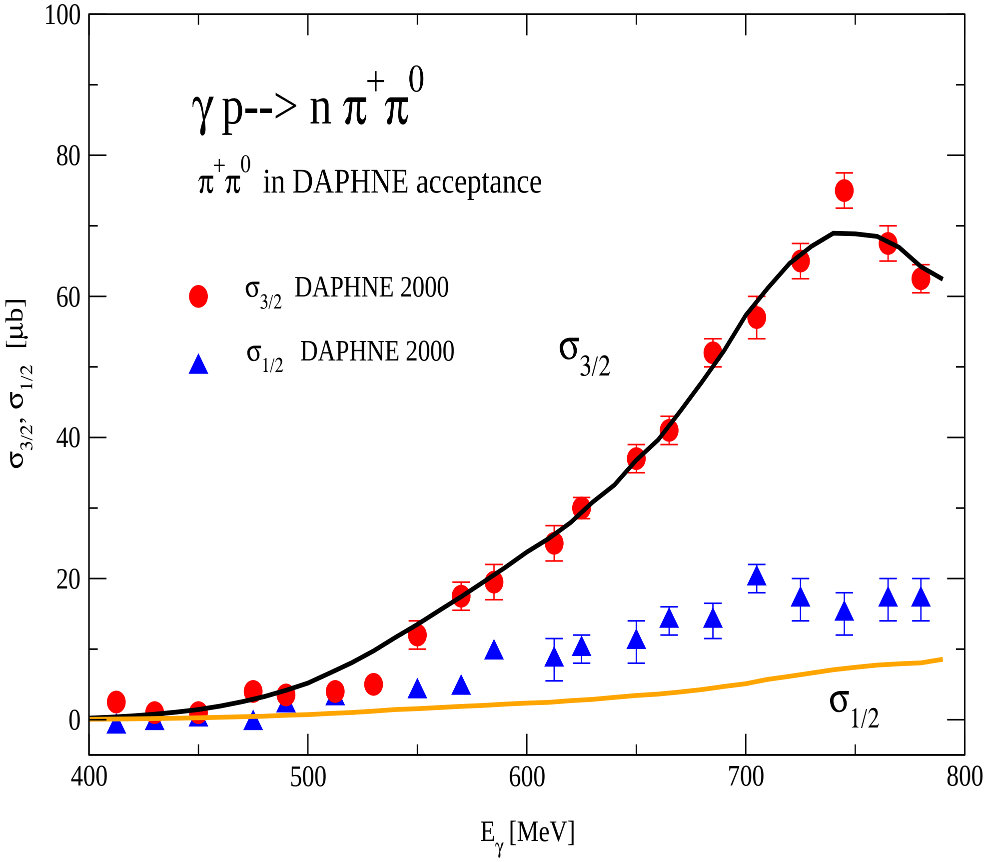

Figure 3: $\sigma_{3/2}$, $\sigma_{1/2}$ for $\vec{\gamma}\vec{p} \to n\pi^+\pi^0$ with $\pi^+\pi^0$ in the DAPHNE acceptance. Experimental data from [16]

In fig. 3 we show the results for the helicity cross section $\sigma_{3/2}$ with a dark continuous line, which are in good agreement with the experimental results. In the case of the $\sigma_{1/2}$ we show the results in a light continuous line and they are somewhat smaller than the experimental numbers.

In view of these results the small deficit of the theoretical cross section in this channel found in [17] should be attributed to the smaller theoretical cross section found for $\sigma_{1/2}$.

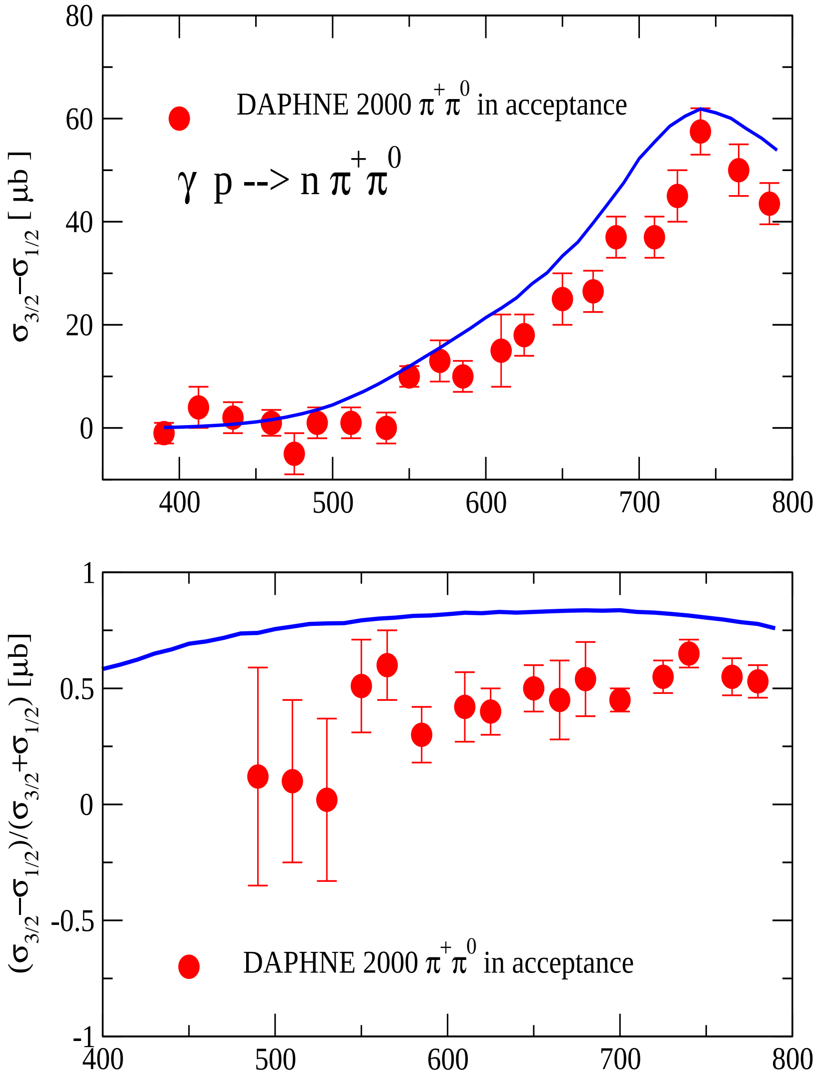

Figure 4: The difference of cross sections $\sigma_{3/2}$ - $\sigma_{1/2}$, for the $\vec{\gamma}\vec{p} \rightarrow n\pi^+\pi^0$ reaction with $\pi^+\pi^0$ in DAPHNE acceptance, is shown in the top figure and the helicity asymmetry in the bottom one. Experimental data from [16]

.

In fig. 4 we show the difference between the helicity cross sections $\sigma_{3/2}$ and $\sigma_{1/2}$ at the top of the figure. In the bottom we show the helicity asymmetry for the $\vec{\gamma}\vec{p} \rightarrow n\pi^+\pi^0$ with $\pi^+\pi^0$ particles in the DAPHNE acceptance. We find good agreement for the $\sigma_{3/2}$-$\sigma_{1/2}$ cross section but we realize that if our $\sigma_{1/2}$ helicity amplitude was a little bit bigger the agreement would be better. At the bottom of fig.4 we can see the results for the helicity asymmetry. We find agreement with the sign of the asymmetry and the global behavior of the observable but the strength of our results has a discrepancy of about a 10% with the data.

3 The GDH Sum Rule for $\gamma p \to \pi\pi N$

The Drell-Hern-Gerasimov (DGH) sum rule relates the helicity structure of the photo absorption cross section to the anomalous magnetic moment. Our aim is to study the convergence of this sum rule in the two pion charged photoproduction reaction.

We write the DHG sum rule (Drell and Hearn, 1966 [20]; Gerasimov, 1966 [21]) as:

$$\frac{\kappa^2}{4} = \frac{m^2}{8\pi^2\alpha} \int \frac{d\nu}{\nu}[\sigma_{3/2}(\nu) - \sigma_{1/2}(\nu)] = I^{GHD}(Q^2 = 0) \quad (9)$$

and $\nu = E_\gamma^{lab}$ photon lab energy. We studied in the last section the helicity observables needed to calculate this expression. We also note that the vector polarizability may be related to another sum rule as [13]:

$$\gamma = \frac{1}{4\pi^2} \int \frac{d\nu}{\nu^3}(\sigma_{3/2} - \sigma_{1/2}) \quad (10)$$

It is interesting to keep in mind that the helicity cross sections are related to the total transverse (σ_T) and transverse-transverse ($\sigma_{TT'}$) cross sections.

$$\sigma_T = \frac{\sigma_{3/2} + \sigma_{1/2}}{2} \quad (11)$$

$$\sigma_{TT'} = \frac{\sigma_{3/2} - \sigma_{1/2}}{2} \quad (12)$$

We show in the fig. 5, from up to down, the difference of the helicities $\sigma_{3/2}$-$\sigma_{1/2}$ and the integrand of the GHD sum rule in terms of the laboratory photon energy. In the intermediate figure we show the integrand of the I^{GHD} sum rule as a function of the photon energy. Finally, we also show a figure at the bottom of fig. 5 the I^{GHD} in terms of the upper limit of photon energy used in the I^{GHD} integral, which seem to indicate that the integral does not converge.

We notice that our model was developed for working in the Mainz range up to 800 MeV photon energy. The result of the I^{GHD} integral up to 800 MeV, lower energy where the model is more reliable, is 0.13 for the $\gamma p \to \pi^+\pi^- p$ reaction. We should note that the value quoted in [13], for the contribution of the $\gamma p \to 2\pi N$ reactions to the I^{GHD} sum rule in [13] from [14] is 0.20, counting all the charged channels. It is worth noting that if we consider the other channels we obtain a contribution from the $\gamma p \to \pi^+\pi^0 n$ channel of 0.07 and from $\gamma p \to \pi^0\pi^0 p$ channel of 0.02 in both cases integrating up to 800 MeV. The total contribution of the $(\gamma, 2\pi)$ channels to the I^{GDH} sum rule up to 800 MeV is 0.22, already larger than the previous estimates, which in principle would account for the integration up to infinite. As an indication of how the GHD sum rule might converge we extrapolate our model up to 1 GeV where

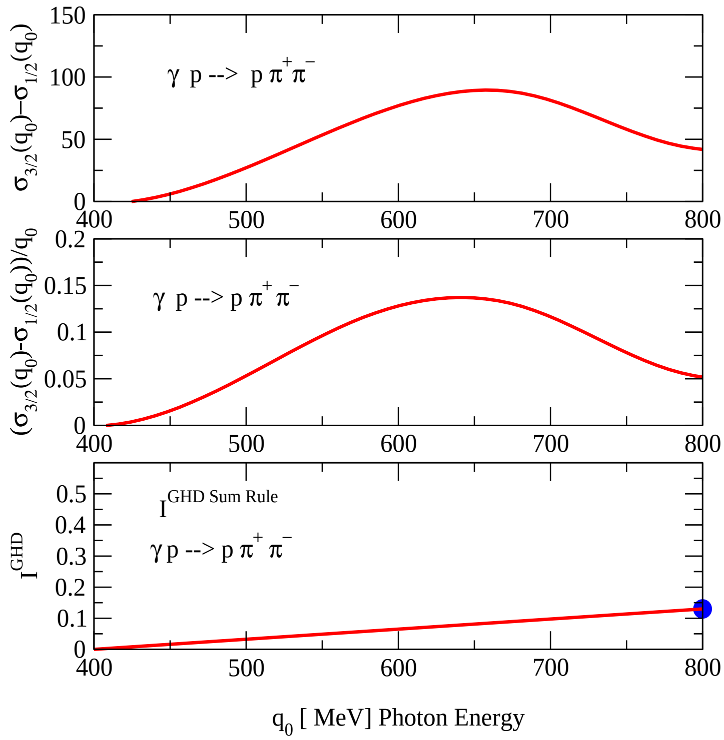

Figure 5: At the top we show the helicity function $\sigma_{3/2}(q_0) - \sigma_{1/2}(q_0)$ in terms of the photon lab energy q_0 up to 800 MeV for the $\gamma p \to \pi^+\pi^- p$ reaction. In the middle figure we show the integrand of the I^{GHD} sum rule $[\sigma_{3/2} - \sigma_{1/2}]/q_0$ up to 800 MeV. At the bottom we show the I^{GHD} sum rule in terms of the photon energy.

the agreement with data should still be fair. We find a contribution to the integral of 0.17, 0.09, 0.02 from the $\pi^+\pi^-$, $\pi^+\pi^0$ and $\pi^0\pi^0$ channel respectively. The sum of all channels is 0.28, which seems an increase of 20 % with respect to the integral up to 800 MeV alone.

We hesitate to use our model at higher energies where it has not been tested against experiment, and where we know that consideration of further resonances and extra unitarity corrections should be important. But the results for the GHD integral shown in fig. 5 and the increase found from 800 MeV to 1000 MeV, do not go in the direction of supporting a fast convergence of this integral. Actually the possibility that the GHD integral does not converge was already advanced in [22].

As with respect to the sum rule for the vector polarizability the fact that we have two extra powers of ν in the denominator increases the chances of convergence. We show in fig. 6 the integrand of eq. (10) for the three charged pion channels and at the bottom of the panel we show the contribution of the integral in terms of the upper limit of integration. The convergence of the $\gamma p \to \pi^+\pi^- p$ and $\gamma p \to \pi^0\pi^0 p$ channels is not fast either and the integral does not seem to saturate around 800 MeV. Furthermore, the $\gamma p \to \pi^+\pi^0 n$ channel shows even a slower convergence. Indeed if we integrate up to 800 MeV the values obtained for the integral are $8.6 \cdot 10^{-5}$ $\mu b/MeV^2$, $4.2 \cdot 10^{-5}$ $\mu b/MeV^2$, $1.3 \cdot 10^{-5}$ $\mu b/MeV^2$ from the $\pi^+\pi^- p$, $\pi^+\pi^0 n$, $\pi^0\pi^0 p$ channels respectively. Altogether we find a contribution to γ from the two pion production channels of 0.00014 $\mu b/MeV^2$ up to 800 MeV. If we integrate up to 1000 MeV then the results are $1.0 \cdot 10^{-4}$ $\mu b/MeV^2$, $6.4 \cdot 10^{-5}$ $\mu b/MeV^2$, $1.7 \cdot 10^{-5}$ $\mu b/MeV^2$ respectively. The sum of all channels up to 1 GeV is 0.00018 μb/MeV^2. However, in spite of this apparent lack of convergence, and admitting that our results at larger energies should overestimate the data, we still find a convergence of the integral around 2 GeV with a value of 0.00030 μb/MeV^2, which we believe is an overestimate of the actual result. Hence we can safely put the results of the 2π channels to the γ sum rule in the range of [0.00018, 0.00030] μb/MeV^2.

4 Polarization asymmetry Σ for two pion photoproduction

For photons linearly polarized in the vertical plane with a polarization degree P, the differential cross section can be written as

$$(\frac{d\sigma}{d\Omega})_{pol}(\theta,\phi) = (\frac{d\sigma}{d\Omega})_{unpol}(\theta)\,(1 + P\Sigma(\theta)cos(2\phi))\,, \quad (13)$$

where ϕ is the angle between the reaction plane and the horizontal plane and $\Sigma(\theta)$ is the beam asymmetry. The cylindrical symmetry of the detector provides the distributions of selected events over the full range $0 - 360$ $[deg]$ of ϕ angles [18].

The asymmetry is extracted experimentally from the azimuthal distribution of events for one of the polarization states, normalized to the azimuthal distribution corresponding to an unpolarized beam.

$$(\frac{d\sigma}{d\Omega})_{pol}(\phi,\theta)/(\frac{d\sigma}{d\Omega})_{unpol}(\theta) = 1 + P\Sigma(\theta)cos(2\phi) = \frac{2F_{ver}(\phi)}{(F_{ver}(\phi) + \alpha F_{hor}(\phi))}\,, \quad (14)$$

where F_{hor} and F_{ver} are the measured azimuthal distributions of events for each polarization state and α is the ratio of beam fluxes corresponding to the vertical and horizontal polarizations. A fit to the experimental data using the function $1 + P\Sigma(\theta)cos(2\phi)$ allows to extract the beam asymmetry $\Sigma = \Sigma(E_\gamma, \theta_{c.m.})$, as a function of the photon energy and the polar angle θ in the centre of mass of the selected particle.

In our case, we implement the calculation of the beam asymmetry Σ in our model with the following prescriptions:

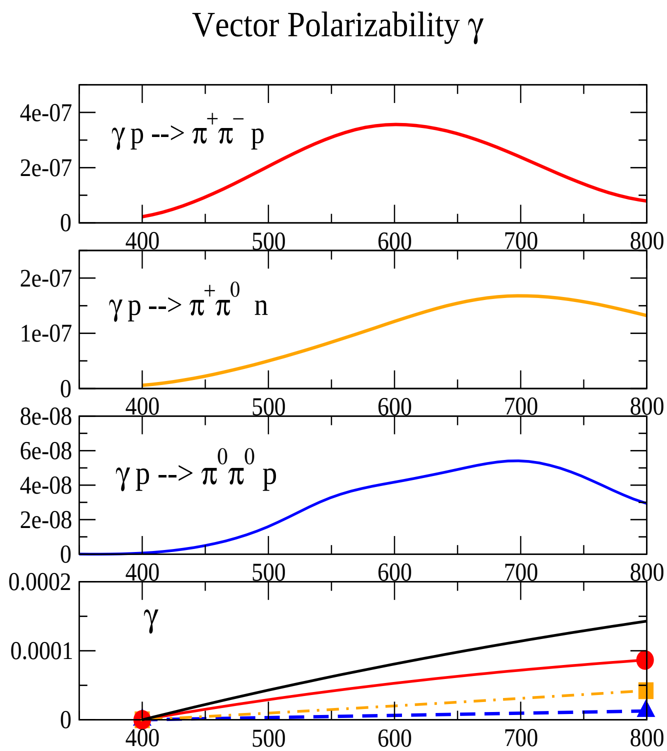

Figure 6: We show the integrand of the vector polarizability γ for the three charged pion channels. At the bottom we show the γ sum rule in terms of the photon energy. for the two pion production channels: (circles) $\pi^+\pi^-$, (squares) $\pi^+\pi^0$, (triangles) $\pi^0\pi^0$. The upper continuous line shows the total sum for the vector polarizability sum rule coming from the three channels.

- The photon momenta is taken in the positive z direction and the x and z axes define the horizontal plane. The vertical polarization goes along the positive y axis and the horizontal polarization along the x axis.
- The reaction plane which contains the momenta of the final particles, defines an azimuthal angle ϕ_R with respect to the initial plane, rotating around the direction z of the incoming photon (z axis).
- Since the only ϕ dependence of the cross section comes from the factor $cos(\phi)$ in eq. (13), we evaluate $\Sigma(\theta)$ choosing $\phi = 0$. For this purpose we select small ϕ_R angles, thus having the final particles essentially in the horizontal plane.

- The asymmetry Σ in our case is defined by

$$\Sigma = \frac{\sigma_T - \sigma_L}{\sigma_T + \sigma_L} \tag{15}$$

  where σ_T corresponds to photons polarized along the y axis while σ_L corresponds to photons polarized in the x axis.

- In a $\gamma p \to N\pi_1\pi_2$ reaction we consider two kind of plots for each channel. We calculate the beam asymmetry for the emission of the system of two pions $(\pi_1\pi_2)$ against the $\theta_{c.m.}$ of the two pions in the global $C.M.$ (case $\gamma p \to\ N\,(\pi_1\pi_2)$). In this case we will show the results selecting the peak of invariant mass of $(\pi_1\pi_2)$ system for several cuts and without cuts.

- The other case is where we calculate the beam asymmetry for the π_1 (or π_2) emission against the $\theta_{c.m.}$ of π_1 (π_2) in the global CM of the reaction (case $\gamma p \to\ (N\pi_2)\,\pi_1$) or $(\gamma p \to\ (N\pi_1)\,\pi_2)$. In these situations we select the peak in the invariant mass of the $(N\pi)$ system around the masss of the Δ resonance. The results without these cuts are also analyzed. This $\theta_{c.m.}$ is defined by the angle between the photon (z direction) and the momentum of the emitted selected particle.

  The selection of cuts discussed above are set up for a future comparison with data presently been taken at GRAAL [19].

In the next pages we can see our predictions for these observables. From fig. 7-13 we analyze the three possible isospin channels with a proton in the initial state, $\gamma p \to \pi^+\pi^-$, $\gamma p \to \pi^0\pi^0 p$, and $\gamma p \to \pi^+\pi^0 n$ reactions. We show the beam asymmetry in several cases, selecting one or two pions and with or without cuts in the invariant masses of the systems.

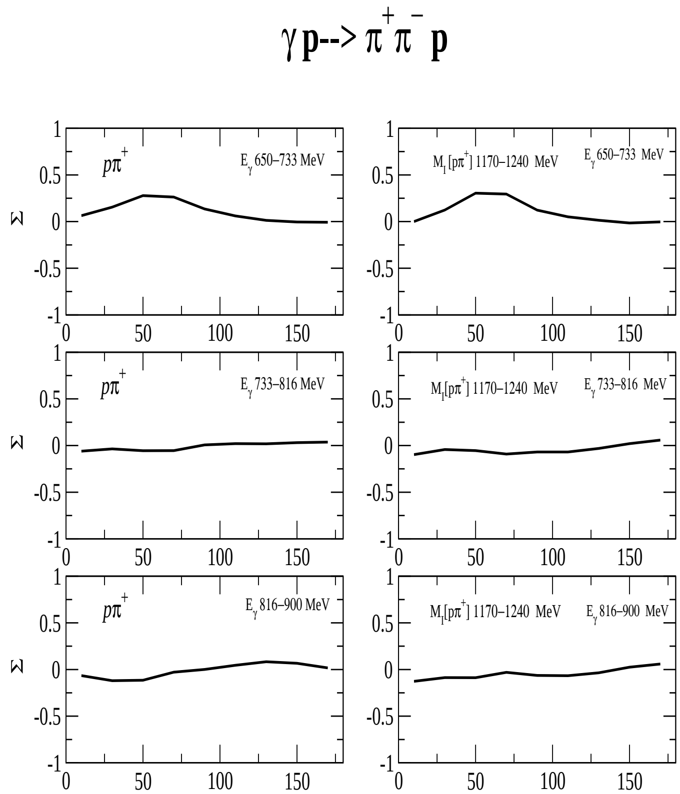

Figure 7: We show the photon asymmetry Σ for the π^- emission against $\theta_{c.m.}$ of π^- in the global C.M. of the reaction $\gamma p \to \pi^+\pi^- p$. The left column shows the beam asymmetry without cut in the invariant masses of the system $(p\pi^+)$. The right column shows the beam asymmetry when we select the peak in the invariant mass of $(p\pi^+)$ system with a band of 1170-1240 MeV (peak around the mass of Δ resonance).

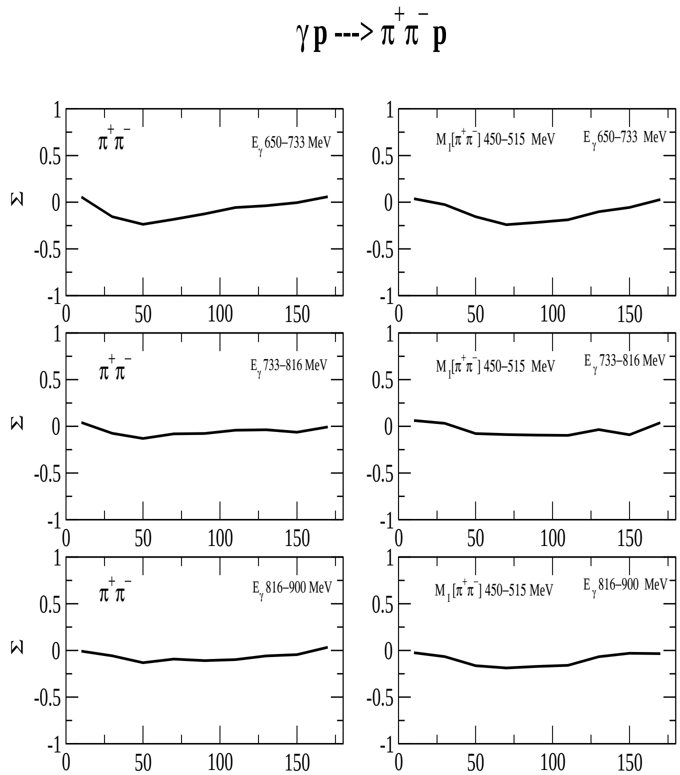

Figure 8: We show the photon asymmetry Σ for the emission of the system of two pions $(\pi^+\pi^-)$ against $\theta_{c.m.}$ of the total momentum of the two pions in the global C.M. of the reaction $\gamma p \to \pi^+\pi^- p$. The left column shows the beam asymmetry without cut in the invariant masses of the system $(\pi^+\pi^-)$. The right column shows the beam asymmetry when we select the peak in the invariant mass of $(\pi^+\pi^-)$ system within a band of 450-515 MeV.

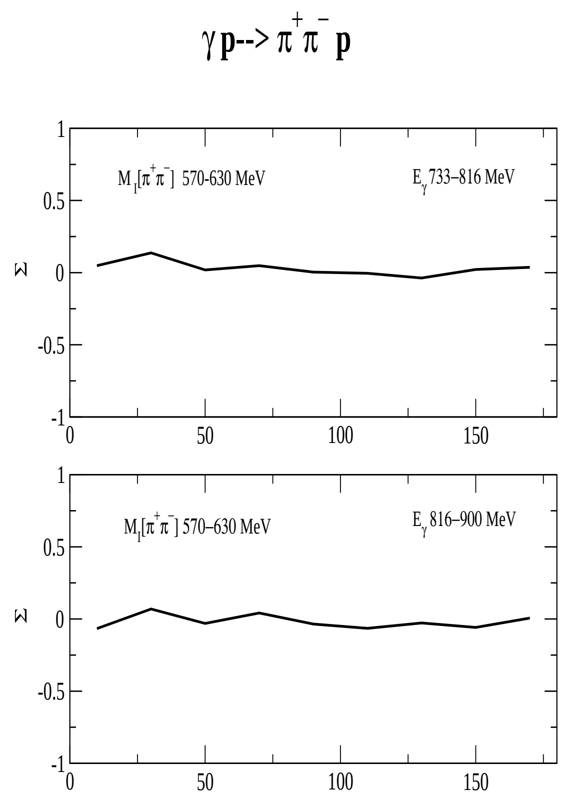

Figure 9: We show the photon asymmetry Σ for the emission of the system of two pions $(\pi^+\pi^-)$ against $\theta_{c.m.}$ of the total momentum of the two pions in the global C.M. of the reaction $\gamma p \to \pi^+\pi^- p$. The column shows the beam asymmetry when we select the peak in the invariant mass of $(\pi^+\pi^-)$ system within a band of 570-630 MeV.

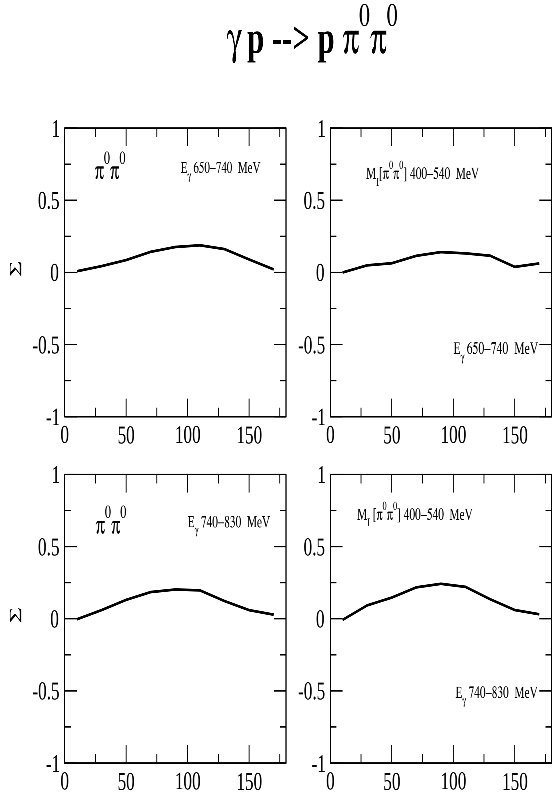

Figure 10: We show the photon asymmetry Σ for the emission of the system of two pions ($\pi^0\pi^0$) against $\theta_{c.m.}$ of the total momentum of the two pions in the global C.M. of the reaction $\gamma p \to \pi^0\pi^0 p$. The left column shows the beam asymmetry without cut in the invariant masses of the system ($\pi^0\pi^0$). The right column shows the beam asymmetry when we select the peak in the invariant mass of ($\pi^0\pi^0$) system within a band of 400-540 MeV.

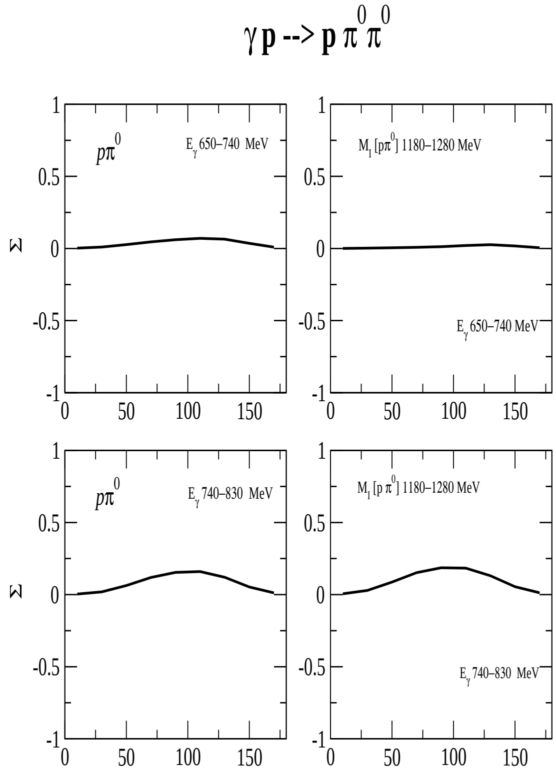

Figure 11: We show the photon asymmetry Σ for the emission of the π^0 pion against $\theta_{c.m.}$ of the π^0 pion in the global C.M. of the reaction $\gamma p \rightarrow \pi^0\pi^0 p$. The left column shows the beam asymmetry without cut in the invariant masses of the system $(p\pi^0)$. The right column shows the beam asymmetry when we select the peak in the invariant mass of $(p\pi^0)$ system within a band of 1180-1280 MeV (peak around the mass of Δ resonance).

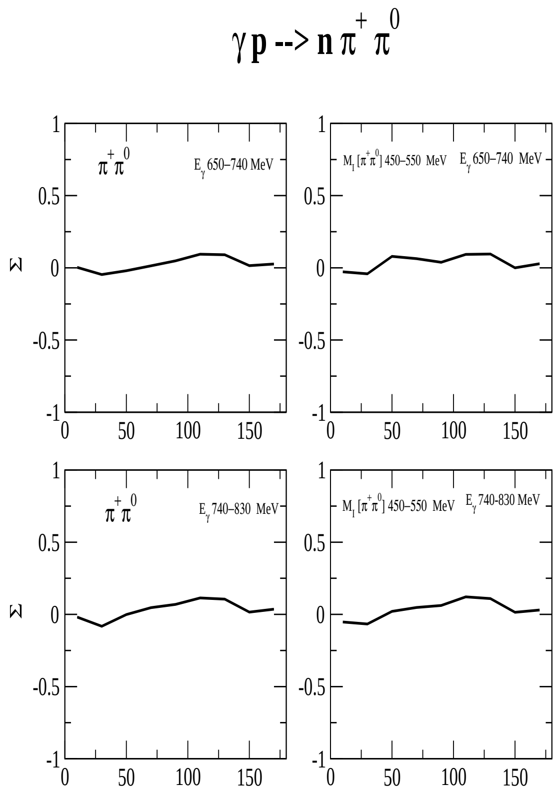

Figure 12: We show the photon asymmetry Σ for the emission of the system of two pions $(\pi^+\pi^0)$ against $\theta_{c.m.}$ of the total momentum of the two pions in the global C.M. of the reaction $\gamma p \rightarrow \pi^+\pi^0 n$. The left column shows the beam asymmetry without cut in the invariant masses of the system $(\pi^+\pi^0)$. The right column shows the beam asymmetry when we select the peak in the invariant mass of $(\pi^+\pi^0)$ system within a band of 450-550 MeV.

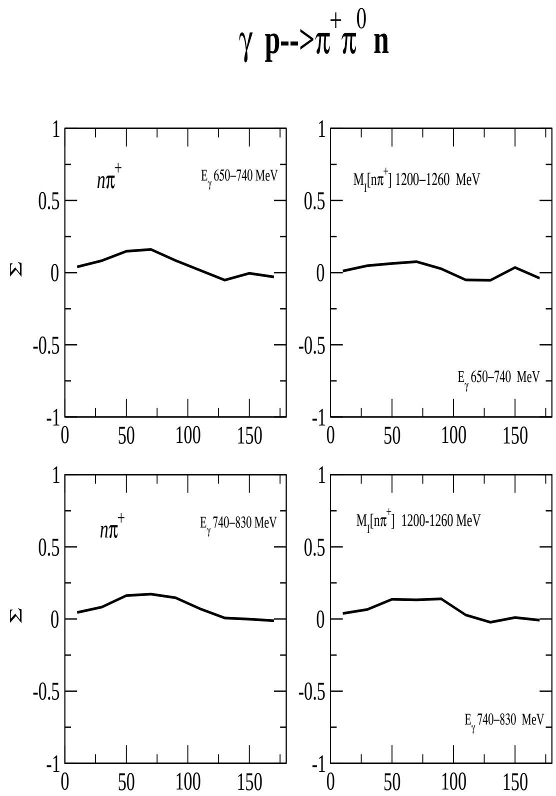

Figure 13: We show the photon asymmetry Σ for the emission of the π^0 pion against $\theta_{c.m.}$ of the π^0 pion in the global C.M. of the reaction $\gamma p \rightarrow \pi^+\pi^0 n$. The left column shows the beam asymmetry without cut in the invariant masses of the system $(n\pi^+)$. The right column shows the beam asymmetry when we select the peak in the invariant mass of $(n\pi^+)$ system within a band of 1200-1260 MeV (peak around the mass Δ resonance).

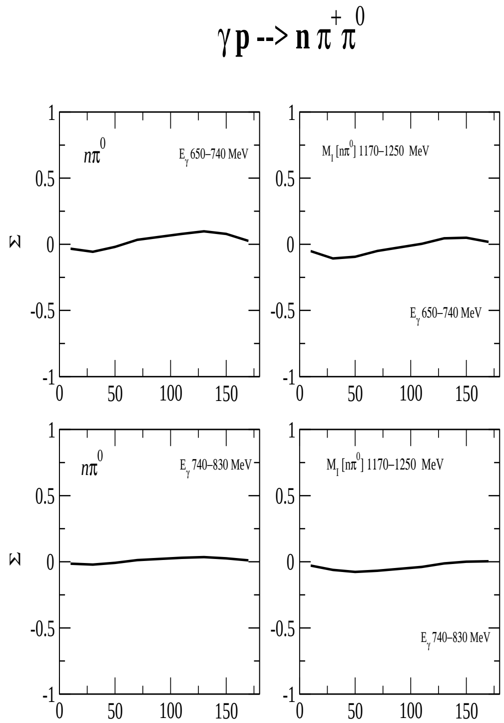

Figure 14: We show the photon asymmetry Σ for the emission of the π^0 pion against $\theta_{c.m.}$ of the π^+ pion in the global C.M. of the reaction $\gamma p \to \pi^+\pi^0 n$. The left column shows the beam asymmetry without cut in the invariant masses of the system $(n\pi^0)$. The right column shows the beam asymmetry we select the peak in the invariant mass of $(n\pi^+)$ system within a band of 1170-1250 MeV (peak around the mass of Δ resonance).

5 Conclusions

We have looked in this paper at the polarization obervables $\sigma_{3/2}$, $\sigma_{1/2}$ and the asymmetry Σ using for it the recent model of [17], which improves over the former one of [8] by including mechanisms of the ρ production and $\Delta(1700)$ excitation. Thanks to the new ingredients of the model we could reproduce the $\gamma p \to \pi^+\pi^0 n$ reaction where the old one had problems. In the present paper we have shown that these new ingredients are essential to reproduce the $\sigma_{3/2}$ cross section in that channel. We nevertheless obtain fair results for the $\sigma_{1/2}$ cross section which has a much smaller strength than the $\sigma_{3/2}$ one. The agreement with the data was found acceptable in all the charged pion channels of the $p(\gamma, 2\pi)$ reaction.

We also took advantage of the success of the model to evaluate the contribution of the $(\gamma, 2\pi)$ channels to the GDH sum rule. Integrating up to 800

MeV the integrand of the GHD sum rule we found a value of 0.22. The integral kept increasing as a function of the upper limit of the integration giving hints of a possible nonconvergence of the GDH sum rule. The evidence of these results should not be considered conclusive, given the fact our model has only been tested against experiment in the range up to 800 MeV, but should be taken as indicative that the GDH integral might not be convergent. On the other hand we also calculated the contribution of the $(\gamma, 2\pi)$ channels to the weighted GDH sum rule leading to the vector polarizability γ. Our results supported convergence of this integral but we still found a sizeable contribution to the integral above 800 MeV.

We have also conducted a thorough study of the photon asymmetry, Σ, and have performed calculations adjusting to the running experimental set up at GRAAL. We show here predictions of the model to be compared to experimental data when the analysis is finished. For the time being we just mention that we find an overall agreement with preliminary data from [19].

Acknowledgments We would like to thank M. Lang, J. Ahrens, M. Guidal and E. Hourany for multiple discussions around their preliminary data. This work has been partially supported by DGICYT contract number BFM2000-1326. One of us J.C. Nacher wishes to acknowledge financial support from the Ministerio de Educación y Cultura.

References

[1] A. Braghieri *et al.*, Phys. Lett. B363, 46 (1995).

[2] A. Zabrodin *et al.*, Phys. Rev. C55, 1617 (1997).

[3] F. Harter *et al.*, Phys. Lett. B401, 229 (1997).

[4] M. Wolf et al., Eur. Phys. J. A9 (2000) 5.

[5] W. Langgaertner et al,. submitted to Phys. Rev. Lett. ; S. Schadmand et al., Acta Phys. Polon. B31 (2000) 2431.

[6] L.Y. Murphy and J.M. Laget, DAPHNIA/sphN 95-42, preprint.

[7] J. A. Gomez Tejedor and E. Oset, Nucl. Phys. A571, 667 (1994).

[8] J. A. Gomez Tejedor and E. Oset, Nucl. Phys. A600, 413 (1996).

[9] K. Ochi, M. Hirata and T. Takaki, Phys. Rev. C56 (1997) 1472.

[10] M. Hirata, K. Ochi and T. Takaki, nucl-th/9711017; M. Hirata, K. Ochi and T. Takaki, Prog. Theor. Phys. Vol. 100,

[11] M. Ripani et al., Nucl. Phys. A672 (2000) 220.

[12] J.A. Gómez-Tejedor, F. Cano and E. Oset, Phys. Lett. B379 (1996) 39.

[13] D. Drechsel, Prog. Part. Nucl. Phys. 34, 181 (1995).

[14] I. Karliner, Phys. Rev. D7 (1973) 2717.

[15] H. Arenhovel, G. Kress, R. Schmidt and P. Wilhelm, nucl-th/9701024.

[16] M. Lang, *private communication, 2000* ; M. Lang, *Proceeding for the GHD- and A2-Collaboration*, December 2000. Submitted to World Scientific.

[17] J. C. Nacher, E. Oset, M. J. Vicente and L. Roca, nucl-th/0012065. Nucl. Phys. A in print.

[18] J. Ajaka *et al.* [GRAAL Collaboration], Phys. Lett. B475, 372 (2000).

[19] E. Hourany and M. Guidal, *private communication, 2000* ; Ajaka et al., *Contribution to the proceedings of "14th International Spin Physics Symposium"*, Suita campus, Osaka University, Osaka, Japan. October, 2000. To be published in AIP Proceedings.

[20] S.D. Drell and A.C. Hearn, Phys. Rev. Lett. 16 (1966) 908.

[21] S.B. Gerasimov, Sov. J. Nucl. Phys. 2 (1966) 430.

[22] D. Drechsel, contribution to the Chiral Dynamics 2000 Worshop, TJNAF, Newport News, USA. July 2000.